Probabilistic Safety and Optimal Control for Survival Analysis of *Bacillus subtilis*[☆]

Alessandro Abate[a], John Lygeros[b], Shankar S. Sastry[c]

[a] *Department of Aeronautics and Astronautics*
Stanford University, USA
[b] *Automatic Control Laboratory*
ETH Zurich, Switzerland
[c] *Department of Electrical Engineering and Computer Sciences*
University of California, Berkeley, USA

Abstract

We introduce a methodological framework based on the concepts of safety and optimality to interpret organismal strategies that are intrinsically related to survival behaviors. We focus on the production of the antibiotic subtilin by the bacterium *Bacillus subtilis*, which is one among a set of possible responses to environmental stress that are elicited by the bacterium, and we investigate the activation strategies over the genes involved in the process. We argue that these activation strategies can be synthesized as the outcome of an optimal control problem that yields a survival probability. This optimization procedure is generated from a probabilistic safety problem, which is formally related to the survival probability. We claim that a proper choice of the value function for the optimization problem that encodes the survival analysis can be related to the activation mechanisms for subtilin production.

Key words: Stress response network, Survival analysis, Safety analysis, Optimal control, Stochastic hybrid systems.

[☆]Research supported by the project HYGEIA, FP6-NEST-004995 (European Commission), and by the US NSF grant CCR-0225610. The first author is currently at the Delft Center for Systems and Control, TU Delft, The Netherlands.

Email addresses: a.abate@tudelft.nl (Alessandro Abate), lygeros@control.ee.ethz.ch (John Lygeros), sastry@eecs.berkeley.edu (Shankar S. Sastry)

1. Introduction

Bacillus subtilis has been the object of much experimental work. The investigation of its stress response network offers a detailed explanation of how the bacterium reacts to adverse environmental conditions [19]. One of the many options available to *B. subtilis* cells is the production of the antibiotic subtilin. The subtilin production pathway has been studied both in its genetics as well as at its signaling level. As a result, the biological mechanisms underlying the generation of the antibiotic subtilin are fairly well understood. The activation/deactivation of the genes involved in the process and the abrupt increase/decrease in the level of the corresponding proteins, which initiate the production of the antibiotic, are often interpreted and modeled by the presence of switching behaviors [18, 24, 25]. These switching mechanisms are associated to stress factors [2, 19], and have been explained through structural [4, 14, 22, 27] and survival arguments [13].

The concept of *optimum* is common and shared between engineering and biological systems [3]. The biology literature offers numerous examples where optimality appears to regulate a certain function, or to explain the properties of a particular entity. [21] represents possibly the first attempt to systematically frame the concept of optimality in biology. An optimality interpretation in the context of metabolic networks is used in [23], whereas [29] looks at dynamical game theory as a means of optimality in the context of evolution, both at the population level and at the cell level. In [17] optimality is related to the notion of stability of a strategy. On the other hand, many notable instances from the same biological domain also caution about the abuse of this notion [10].

Motivated by a recently developed dynamical model [12] for the genetic network that describes the biosynthesis of the antibiotic subtilin by the bacterium *B. subtilis*, the goal of this work is to revisit the concept of optimality and to investigate its use in the study of survival for the bacterium. We put forward a new approach to study and understand the control mechanisms for the production of subtilin, and interpret these mechanisms in terms of an optimization problem.

We first propose a few improvements and modifications to the model in [12], to bring it in line with newer evidence reported in the literature [24, 25, 28]. The overall dynamical model describing the antibiotic production is framed in the context of a Stochastic Hybrid System (SHS) [1]. Our aim is not to shed new light into the actual dynamics of the antibiotic pathway, but rather, given a model, to propose a new approach to study the control mechanisms for the production of subtilin in terms of certain optimality

criteria. The methodology to attain the objective is developed in three

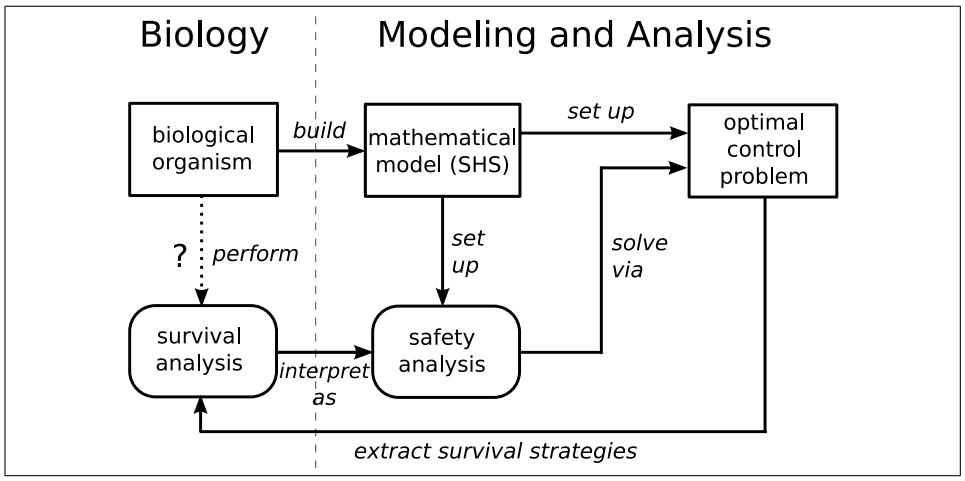

Figure 1: Schematic representation of the methodology. The biology is introduced in Section 1; the mathematical models in Sections 2,3.1; safety analysis and its related optimal control problem in Sections 3.2, 3.3; and the results are discussed in Sections 4 and 5.

steps (Figure 1):

1. We interpret survival analysis as a probabilistic safety analysis problem
2. We deploy optimal control theory tools to solve the safety problem
3. We elucidate its outcomes in relationship to survival analysis

The formal techniques developed in Section 3.2 and based on the SHS model in [1] allow to reinterpret and study the survival analysis, through its connection with probabilistic safety, as a stochastic optimal control problem. In the model the available controls are feedback functions of the state-space and encode the subtilin production strategies: under a proper choice of the survival function, the solution of this optimal control problem obtains what we associate with the location and the structure of the switching (activation/deactivation) behaviors that characterize the subtilin production mechanism. We furthermore draw some comparisons on the outcomes of the above procedure using different survival functions.

This methodological approach, summarized in Figure 1, allows a quantitative study of survival analysis for *B. subtilis* and proposes a procedure to understand its survival strategies. More generally, the study suggests that certain functions in a biological network may be synthesized as solutions of optimization problems, which are based on quantitative models of the dynamics and encode the specific behaviors that the functions elicit.

The article is structured as follows: Section 2 describes the dynamical model for the production biosynthesis of subtilin by *Bacillus subtilis*. Section 3 develops the details of the proposed approach: Section 3.1 reinterprets the model as a Stochastic Hybrid System, Section 3.2 develops a probabilistic safety verification procedure for the introduced model, and Section 3.3 interprets the concept of survival as a safety specification, relating survival to the verification procedure of Section 3.2. Section 4 presents and discusses some numerical results that associate the outcomes of the optimization problem with certain survival strategies. Section 5 outlines a number of directions for future studies.

2. A Model for Antibiotic Biosynthesis

Many biological systems with interacting continuous and discrete components are naturally captured by Hybrid Systems models [7, 9]. The use of such models has indeed been recently advocated in the Systems Biology literature [5, 7, 9, 11, 16, 20]. Along these lines, we introduce in this Section a model for the system under study and interpret it as a SHS in Section 3.1, to further develop some analysis on it in Section 3.2. For a thorough presentation of the SHS framework, the reader is referred to [6].

The model for the antibiotic synthesis is a refinement of that appeared in [12], according to additional evidence on *B. subtilis* [24, 25, 28]. The subtilin biosynthesis network is expressed with two classes of variables (see Figure 2): global/macroscopic variables (population density D and nutrient level X) and local/microscopic ones (the concentration of the sigma factor SigH, denoted with [SigH], and that of the protein SpaS, denoted with [SpaS]). The macro- and microscopic variables interact through the average value of SpaS within the population (denoted as $\overline{[\mathrm{SpaS}]}$) and through an activation function (identified with u) to be defined shortly (Figure 2). For the sake of simplicity the scheme disregards some of the components in the otherwise complex subtilin biosynthesis pathway, as well as some ancillary behavior that is only tangentially of interest at this level. For instance, we disregard the presence of a few peptides that play a role in the immunity response [15, 26, 27], and use the presence of the peptide SpaS to represent the actual antibiotic subtilin. In addition, unlike [12], we do not include the influence of SpaRK, an additional protein in the biosynthesis pathway.

At the microscopic level, we start with the dynamics of SigH, which is thought to be the initiator of the subtilin production pathway. The literature on antibiotic synthesis as a stress response for *B. subtilis* suggests that the activation/deactivation of subtilin production follows a "switching" profile

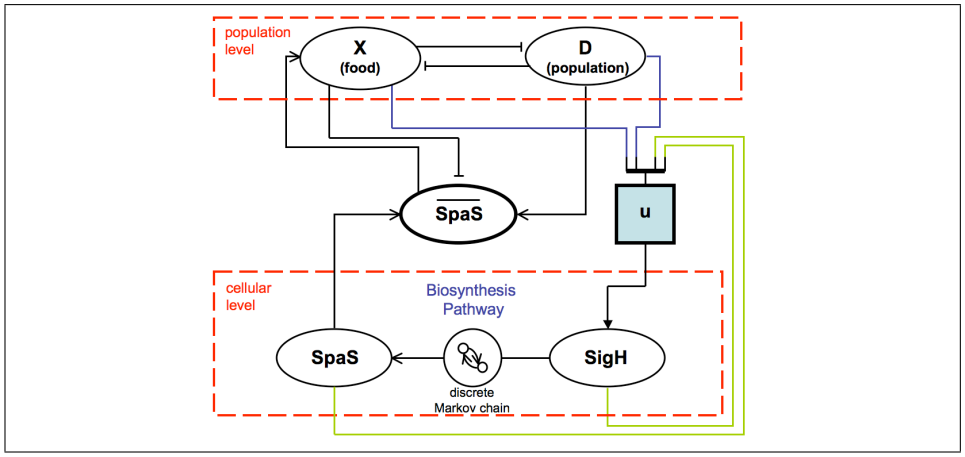

Figure 2: The decentralized structure of the model under study. The top layer (dashed red box above) refers to the population dynamics (nutrient level and population size), which are deterministic. The bottom layer (dashed red box below) refers to the dynamics of a single cell, which are stochastic and hybrid. Pointed arrows ($\rightarrow$) denote direct positive influence, whereas tagged arrows ($\dashv$) denote negative effect. Blue connectors indicate a global influence on the control structure (represented as a light blue box), while green ones the local effect on the control. The control influences (positively or negatively–hence the use of a specific arrow) the concentration of the sigma factor SigH.

[12, 24, 25, 28]. Motivated by this observation, we consider general switching rules of the form:

$$\frac{d[SigH]}{dt} = -\lambda_1[SigH] + k_3 u, \tag{1}$$

where the control u takes binary values as

$$u = f(D, X, [SigH], [SpaS]) : \mathcal{D} \rightarrow \{0, 1\}, \tag{2}$$

with $\mathcal{D} = [0, D_M] \times [0, X_M] \times \mathbb{R}^2_+ \subset \mathbb{R}^4$, and where the quantities D_M, X_M represent saturation levels and will be formally introduced shortly. Notice that we have implicitly assumed a causal and memory-less structure for the controls: to the best of our knowledge, anticipativity (non-causal behavior) has not been observed as of yet in biological systems at that scale, and memory-dependent policies would require an understanding of some sort of memory structure, which the literature presently does not support.

The sigma factor SigH influences the dynamics of the peptide SpaS: the higher the concentration level of SigH, the more likely it is that SpaS is produced. This influence is established through a discrete switching mechanism [12], namely a two-state Markov chain S_1, and influences the continuous dy-

namics of SpaS as follows:

$$\frac{d[SpaS]}{dt} = \begin{cases} -\lambda_3[SpaS] & \text{if } S_1 \text{ is OFF} \\ -\lambda_3[SpaS] + k_5 & \text{if } S_1 \text{ is ON.} \end{cases} \tag{3}$$

$S_1 = \{\text{OFF}, \text{ON}\}$ is assumed to be a Markov chain evolving at constant time interval $\Delta > 0$, and endowed with the following transition probability matrix: $P_1 = \begin{bmatrix} 1-b_0 & b_0 \\ 1-b_0 & b_0 \end{bmatrix}$. The coefficient b_0 depends directly on [SigH] as $b_0([SigH]) = \frac{e^{-\Delta G_{rk}/RT}[SigH]}{1+e^{-\Delta G_{rk}/RT}[SigH]}$. The quantity ΔG_{rk} represents the Gibbs free energy of the molecular configuration, R is a gas constant and T the environment temperature in Kelvin. This choice of P_1 as a transition probability matrix makes S_1 a *reversible* Markov chain with a stationary distribution $[\pi_{OFF}, \pi_{ON}]^T = [1-b_0, b_0]^T$. Intuitively, SigH promotes the production of SpaS by increasing the probability of S_1 to be in the ON state, where the concentration of SpaS grows.

At the macroscopic level of the model, the dynamics of both the population size and the nutrient level are influenced by the average amount of subtilin currently present in the environment. The variation in the population size is modeled by a logistic equation:

$$\frac{dD}{dt} = rD\left(1 - \frac{D}{D_\infty}\right), \quad r > 0. \tag{4}$$

The non-trivial equilibrium depends on the quantity D_∞ (the *carrying capacity*), taken to be equal to $D_\infty = \frac{X}{X_M} D_M$, where D_M and X_M represent the maximal values for the population and the nutrient levels in the environment. The nutrient level dynamics are:

$$\frac{dX}{dt} = -k_1 DX + k_2 \overline{[SpaS]}. \tag{5}$$

The nutrient level decreases at a rate proportional to its present level and to the population density. It furthermore increases at a rate proportional to the average production of subtilin, which is due to the indirect negative influence of the antibiotic on the population level. The average concentration of antibiotic is modeled by:

$$\overline{[SpaS]} = \frac{D}{D_M}\left(1 - \frac{X}{X_M}\right)\frac{k_5}{\lambda_3} b_0 h(X), \tag{6}$$

where b_0 has been defined above and $h(X)$ is equal to 1 if $X > 0$, and to 0 if $X = 0$. The relation in (6) stresses two separate influences: a dependence on

the "competition" in the environment, modeled by the term $\frac{D}{D_M}\left(1-\frac{X}{X_M}\right)$; and one on the steady state dynamics for [SpaS] (fraction k_5/λ_3), which in turn depends on the state of SigH ($\pi_{ON} = b_0(k_3 u/\lambda_1)$, from (1),(3)). In this work the quantity $\overline{[SpaS]}$ has a structure which is more complex than the proportional relation used in [12].

Notice that the macroscopic level of the model, which encompasses the population and nutrient levels, is deterministic and based on average dynamics. The microscopic one, involving the protein and sigma factor concentration levels, describes cellular processes and is made up of stochastic and switching dynamics (concentrated on the switching structure of the Markov chain S_1).

From the dynamical relations in (4),(5) and (6), the steady state $[D_{eq}, X_{eq}]^T$ of the population and nutrient level is going to be either

$$[D_{eq}, X_{eq}]^T = [0, \beta]^T, \beta \in [0, X_M], \text{ or}$$

$$[D_{eq}, X_{eq}]^T = [\alpha D_M, \alpha X_M]^T, \text{ where } 0 < \alpha \leq \frac{k_2 k_3 k_5}{k_2 k_3 k_5 + k_1 \lambda_1 \lambda_3 D_M X_M} \leq 1.$$

It is easy to see that the first equilibrium is unstable, whereas the second is locally stable for any combination of the model parameters. It can be shown that the dynamics belong to the positive quadrant and are upper bounded by the extrema D_M, X_M.

3. Survival Analysis

We recast the above dynamics as a control-dependent SHS model in Section 3.1. The SHS model will enable the application of a control synthesis procedure, described in Section 3.2. We then originally relate such control synthesis to the problem of interest (survival analysis) in Section 3.3.

3.1. Stochastic Hybrid System Model

In order to relate the model in Section 2 to the SHS framework [1], from now on we shall work in discrete time, assuming that the dynamics have been properly approximated, for instance with a first-order forward-Euler time-discretization method with fixed sampling time $\Delta > 0$.

The state space $\mathcal{S}$ of the SHS is made up of a discrete component $q \in \{\text{OFF}, \text{ON}\}$ (the state of S_1), and a continuous one $x \in \mathcal{D} \subset \mathbb{R}^4$, as in (2). We use the product $\mathcal{S} = \{\text{OFF}, \text{ON}\} \times \mathcal{D}$ to denote the hybrid state space. The dynamics of the continuous variables are characterized by the relations

in (1),(3),(4), and (5). In particular, SigH depends on a binary function that expresses, according to (2), a general feedback contribution from the hybrid state space $\mathcal{S}$.

The solution of the above SHS model over a time horizon $[0, N]$ is a stochastic process with two components $\mathbf{s}(k) = (\mathbf{q}(k), \mathbf{x}(k)), k \in [0, N]$[1] [1, Def. 3]. Given an initial condition at time $k = 0$, the solution evolves in either of the two discrete modes until a mode switch is verified (which reduces to sampling, along the evolution of the trajectory, from the non-homogeneous probability distribution of the Markov chain S_1). Once a transition is triggered, the discrete state changes mode and the continuous evolution proceeds from unaltered initial conditions within the new mode. By construction, given the structure of the binary control and its sole dependence on the present state at each time step, once a control function is selected the solution process is Markovian (that is, memory-less).

The discrete and finite control space is denoted with $\mathcal{U} = \{0, 1\}$. As in [1, Section 4.2], we call a *strategy*, or a *policy*, a control profile over a certain finite time horizon $[0, N]$, that is a sequence of N mappings $\mu = (u_0, u_1, \ldots, u_{N-1}) \in \mathcal{U}^N, u_k : \mathcal{D} \to \mathcal{U}$, as in (2).

Finally, to be able to formally state the technical result in Theorem 1 on page 9, let us introduce a stochastic kernel $T_s : \mathcal{B}(\mathcal{S}) \times \mathcal{S} \times \mathcal{U} \to [0, 1]$ on $\mathcal{S}$ given $\mathcal{S} \times \mathcal{U}$, which assigns to any point $s = (q, x) \in \mathcal{S}$ and control $u \in \mathcal{U}$, a probability measure on the Borel space $\mathcal{B}(\mathcal{S})$, according to the dynamics of the SHS. The kernel T_s defines the dynamical behavior of the SHS, and this mapping is probabilistic because of the presence of the Markov chain S_1.

3.2. Safety Verification for Stochastic Hybrid Systems

The safety verification analysis in this Section relates the SHS model of Section 3.1 with the issue of survival analysis discussed in Section 3.3.

In general terms, in a stochastic setting a *safety verification* problem consists in evaluating the probability that the state of the system remains inside a certain set deemed to be *safe* during a given time horizon, starting from some initial conditions within that set. More formally, for a given initial state $s_0 \in \mathcal{S}$, a Markov policy $\mu \in \mathcal{U}^N$, and a (safe) set $\mathcal{A} \subseteq \mathcal{S}$, it is of interest to compute the probability that the execution associated with the policy μ and with initialization in s_0 stays within $\mathcal{A}$ during the time $[0, N]$:

$$\mathrm{p}^{\mu}_{s_0}(\mathcal{A}) := \mathcal{P}(\mathbf{s}(k) \in \mathcal{A}, \text{ for all } k \in [0, N] | \boldsymbol{s}(0) = s_0). \tag{7}$$

[1]Bold symbols are used to denote processes, whereas normal typeset to denote points or sample values in the (hybrid) state space.

The set $S^{\mu}(\epsilon)$ of initial conditions guaranteeing a safety level $\epsilon \in [0,1]$, when the control policy $\mu \in \mathcal{U}^N$ is assigned, $S^{\mu}(\epsilon) = \{s \in \mathcal{S} : \mathrm{p}_s^{\mu}(\mathcal{A}) \geq \epsilon\}$, is referred to as the *probabilistic safe set* with safety level ϵ. Notice that the set $S^{\mu}(\epsilon)$ depends on a particular policy $\mu \in \mathcal{U}^N$. It is then of interest to pick an "optimal" policy leading to the set $S^{\star}(\epsilon) = \{s \in \mathcal{S} : \max_{\mu \in \mathcal{U}^N} \mathrm{p}_s^{\mu}(\mathcal{A}) \geq \epsilon\}$, called the *maximal probabilistic safe set*. A policy $\mu^{\star} \in \mathcal{U}^N$ is *maximally safe* if $\mathrm{p}_s^{\mu^{\star}}(\mathcal{A}) = \max_{\mu \in \mathcal{U}^N} \mathrm{p}_s^{\mu}(\mathcal{A})$, $\forall s \in \mathcal{A}$. The maximal probabilistic safe set and the maximally safe policy can be computed using tools from optimal control (see [1] for a complete treatment).

Let $\mathbf{1}_{\mathcal{A}} : \mathcal{S} \to \{0,1\}$ denote the indicator function of set $\mathcal{A} \subseteq \mathcal{S}$. Regard a given set of $N+1$ points $\{s_k\}$ to be a realization of the process $\boldsymbol{s}(\cdot)$, according to a particular policy $\mu \in \mathcal{U}^N$ and with initialization in $s_0 \in \mathcal{S}$. Observe that

$$\prod_{k=0}^{N} \mathbf{1}_{\mathcal{A}}(s_k) = \begin{cases} 1, & \text{if } s_k \in \mathcal{A}, \text{ for all } k \in [0,N] \\ 0, & \text{otherwise.} \end{cases}$$

It follows that

$$\mathrm{p}_{s_0}^{\mu}(\mathcal{A}) = \mathcal{P}\left(\prod_{k=0}^{N} \mathbf{1}_{\mathcal{A}}(\mathbf{s}(k)) = 1 | \, \mathbf{s}(0) = s_0 \right) = E\left[\prod_{k=0}^{N} \mathbf{1}_{\mathcal{A}}(\mathbf{s}(k)) | \, \mathbf{s}(0) = s_0 \right].$$

This expression suggests that the quantity $\mathrm{p}_{s_0}^{\mu}(\mathcal{A})$ can be computed through a backward iterative procedure, as detailed in the following. For each $k \in [0,N]$, define the map $V_k^{\mu} : \mathcal{S} \to [0,1]$ by:

$$V_k^{\mu}(s) = E\left[\prod_{l=k}^{N} \mathbf{1}_{\mathcal{A}}(\mathbf{s}(l)) | \, \mathbf{s}(k) = s \right],$$

with $V_N^{\mu}(s) = \mathbf{1}_{\mathcal{A}}(s)$. This map denotes the probability of remaining inside $\mathcal{A}$ during the (residual) time horizon $[k,N]$ starting from a specific $s \in \mathcal{S}$ at time k, under the relevant part of the policy μ. It follows that, for any $s \in \mathcal{S}, \mathrm{p}_s^{\mu}(\mathcal{A}) = V_0^{\mu}(s)$. The following theorem describes an algorithm to compute the quantity $\max_{\mu \in \mathcal{U}^N} \mathrm{p}_s^{\mu}(\mathcal{A})$ and ensures the existence of a maximally safe policy $\mu^{\star} \in \mathcal{U}^N$.

Theorem 1 ([1], Theorem 1). *Define the maps $V_k^{\star} : \mathcal{S} \to [0,1]$, $k = 0, 1, \ldots, N$, with $s \in \mathcal{S}$, by the backward recursion:*

$$V_k^{\star}(s) = \max_{u \in \mathcal{U}} \boldsymbol{1}_{\mathcal{A}}(s) \int_{\mathcal{S}} V_{k+1}^{\star}(s_{k+1}) T_s(ds_{k+1} | s, u),$$

initialized with $V_N^\star(s) = \mathbf{1}_{\mathcal{A}}(s)$. *Then,* $V_0^\star(s) = \max_{\mu \in \mathcal{U}^N} \mathrm{p}_s^\mu(\mathcal{A}), \forall s \in \mathcal{S}$. *Moreover, there exists a maximally safe policy* $\mu^\star = (u_0^\star, \ldots, u_{N-1}^\star)$, *with* $u_k^\star : \mathcal{S} \to \mathcal{U}$, $k \in [0, N-1]$, *given* $\forall s \in \mathcal{S}$ *by*

$$u_k^\star(s) = \arg\max_{\mu \in \mathcal{U}} \mathbf{1}_{\mathcal{A}}(s) \int_{\mathcal{S}} V_{k+1}^\star(s_{k+1}) T_s(ds_{k+1}|s, u).$$

□

The procedure in Theorem 1 can be implemented via a dynamic programming algorithm on a discretization of the state space, as discussed in [1].

3.3. Survival Analysis as a Probabilistic Safety Verification

According to the biological interpretation discussed in Section 1 and to support from the literature on *B. subtilis* [13, 19], it is assumed that an organism activates or deactivates the "production pipeline" for the antibiotic subtilin with the main objective of maximizing its own probability of survival. It is possible to reinterpret the survival objective as a safety specification by introducing appropriate safety regions within the state space and using the machinery developed in Section 3.2 to compute and maximize the associated safety probabilities. The validity of this procedure, schematically recapitulated in Figure 1, clearly hinges on the relationship between survival and safety. If the survival mechanism is expressed in terms of the variables of the model, this connection is immediate. A number of educated guesses on the proper relationship between survival and safety for the instance under study are introduced below and tested numerically in Section 4.

Interpreting the survival mechanism that leads to the production of the antibiotic subtilin as a stress response (as discussed in the Introduction and in Section 2), we can regard safety as the verification of the following condition:

$$\text{" safe if } [SpaS] > \overline{[SpaS]} \text{ "} \tag{8}$$

Informally, (8) says that if the subtilin production level for a cell is higher than the average level of antibiotic present in the environment, then the organism is deemed to be safe: (8) encodes a higher probability for the organism to kill other bacteria, rather than being killed by their antibiotic production. By (6) and (8), the associated *safe region*, called $\mathcal{A}_1$, is then:

$$\mathcal{A}_1 = \left\{ s \in \mathcal{S} : [SpaS] > \frac{D}{D_M} \left(1 - \frac{X}{X_M}\right) \frac{k_5}{\lambda_3} b_0 h(X) \right\}.$$

We additionally designate a second survival mechanism, which depends on a simple feedback structure that accounts for the competition coming from

the environment. This second feedback corresponds to the observation that the bacterium adjusts its behavior according to *quorum sensing* [12, 28], that is according to a global measure of population or nutrient level:

" safe if nutrient level is high or if population density is low " (9)

Accordingly, the second safe region $\mathcal{A}_2$ is defined to be the set of points:

$$\mathcal{A}_2 = \left\{ s \in \mathcal{S} : \frac{D}{D_M}\left(1 - \frac{X}{X_M}\right) < \texttt{thresh} \right\}, 0 \leq \texttt{thresh} \leq 1.$$

Recall that the subtilin level influences the nutrient level and indirectly also the population level. Finally, let us consider a safety condition defined over the nutrient level, as suggested in [12]:

" safe if nutrient level is higher than threshold " (10)

Accordingly, the third safe set $\mathcal{A}_3$ has the following shape:

$$\mathcal{A}_3 = \left\{ s \in \mathcal{S} : \frac{X}{X_M} > \texttt{thresh} \right\}, 0 \leq \texttt{thresh} \leq 1.$$

The application of the procedure described in Theorem 1 computes the optimal policies for the safety sets selected above. This output represents the synthesized control feedback functions for the relation in (1). We expect to be able to associate the presence of activation/deactivation thresholds (which represent a "switching" behavior) for the production of subtilin to a particular survival mechanism.

4. Numerical Results and Discussion

We have selected the following parameters for the dynamics introduced in Section 2: $r = 0.8, k_1 = 2, k_2 = 4, k_3 = 2.5, k_5 = 0.8, \lambda_1 = 0.5, \lambda_3 = 0.2, \Delta G_{rk}/RT = 1.1$. The time horizon for the optimization problem has been set to $N = 40$, which allows to assess the dynamics and the structure of the synthesized controls in their steady state. We have first considered the safety condition expressed in (8), its corresponding safety set $\mathcal{A}_1$, and performed the computations as in Theorem 1 after discretizing uniformly the state space. In Figure 3, the plots of the maximal probabilistic safety *level sets*, with safety level $\epsilon = 0.95$, are shown for a few different time samples (initial time on the left, transient centrally, steady state on the right). Colored hues have been added only to enhance the perspective and

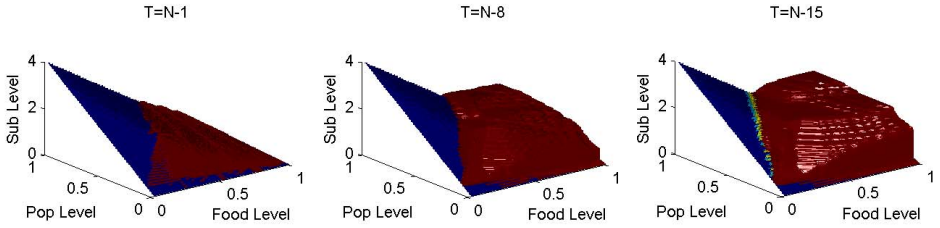

Figure 3: Maximal probabilistic safety level set corresponding to $\epsilon = 0.95$ for different time samples (initial time on the left, transient centrally, steady state on the right). The points above the level surfaces are safe with a probability of at least 95%. The sigma factor level has been fixed to [SigH] = 1, the discrete state is in the OFF mode. The coordinates represent horizontally the nutrient level X and the population density D, and vertically the level of subtilin [SpaS].

the height of the level curves. The maximal probabilistic safe sets are thus made up of the points *above* the plotted level curves. More precisely, given the choice of the safety level ϵ, all the points in the plots above the level surfaces are considered to be safe with a probability of at least 95%. For the sake of visualization (being the continuous state space four-dimensional), we plotted the results corresponding to a fixed value of the sigma factor [SigH] = 1 (the three dimensions represent the nutrient level $X \in [0, X_M]$ and the population level $D \in [0, D_M]$ on the horizontal plane, and the level of subtilin $[SpaS] \geq 0$ on the vertical axis), and the discrete state being in the OFF mode. Results that are similar to those displayed, in that they single out a distinct partition of the state space, are obtained for other choices of coordinates, and analogous outputs are displayed for the ON mode. In Figure 3 notice that, as expected, the safe set shrinks (that is, the curve raises) as we proceed backwards in time (towards the steady state condition): this in fact translates to a longer safety requirement for the trajectories of the system.

Figure 4 shows the different maximal probabilistic safety level sets at steady state for a few values of the safety probability ϵ (decreasing towards the right). As expected, the lower the probabilistic safety level, the lower the level surface, and the larger the safety region.

Finally, Figure 5 represents vertical pairs of plots referring to maximal probabilistic safety level sets (for $\epsilon = 0.95$, in the top row) and corresponding optimal actions (bottom row), for a few different time samples (initial time on the left, transient in the center, and steady state on the right). More precisely, the plots on the top row are obtained similarly as Figure 3, whereas the plots on the bottom row represent the regions in the state space that

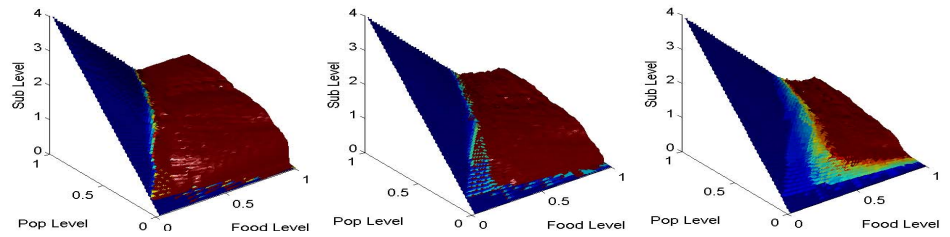

Figure 4: Maximal probabilistic safety level set corresponding to different safety levels (decreasing along the left-right direction: $\epsilon = 0.9, \epsilon = 0.5, \epsilon = 0.1$) for a particular time sample (in steady state): the points above the level surfaces are safe with a probability of at least $100\epsilon\%$. The spatial coordinates are organized as in Figure 3.

are associated with a *switching condition* over the binary control (that is, where the control commutes as OFF $\rightarrow$ ON or as ON $\rightarrow$ OFF), and are to be matched with the safety level sets plotted directly above them.

Central to the argument of this work, it is interesting to realize that the optimal control functions that are associated with the activation/deactivation conditions for the production of the antibiotic (that is, the set of points associated with a binary switch of the control u in (2)) have a characteristic "onion layer" shape that varies in time and is concentrated on a surface. It can be thus asserted that the optimal controls synthesized by the problem according to the specific survival specification single out switching surfaces corresponding to certain safety levels. These surfaces have profiles that follow the variation in safety probability (or, according to our interpretation, in survival probability) for the bacterium, as appears by comparing the curves for the switching control with the safety level sets plotted above them in Figure 5. Notice that in general these surfaces are not hyper-rectangular, as assumed in [8, 12], which also sought to identify the production thresholds. Instead, they are rather nonlinear functions of the state space, showing a manifest but non-explicit dependence with the change in safety level of the single organism.

The simulations based on the second survival condition expressed in (9) are important to rule out "false positives" for the proposed procedure. We have experimented a number of threshold levels and report here the outputs for `thresh` $= 0.3$. The outcomes of the simulations are shown in Figure 6. Notice that the survival probabilities (top plots) and the optimal actions (bottom plots) are now interpreted as curves, rather than level sets (as in Figures 3, 4, and 5), because of the lower dimensionality (two, rather than

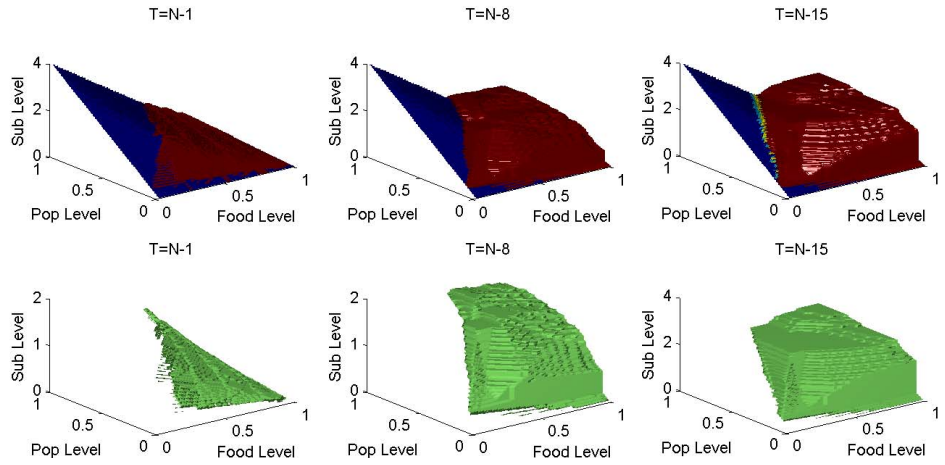

Figure 5: Maximal probabilistic safety level sets and optimal switching control, for a few time samples (initial time on the left, transient centrally, steady state on the right) and a safety level $\epsilon = 0.95$. On the top row, the points above the level surfaces are safe with a probability of at least 95%. On the bottom row, the curves represents points in the state space that are associated with a switching condition. The spatial coordinates are organized as in Figure 3.

four) of the figure of merit in $\mathcal{A}_2$. While the safety levels appear to remain similar in time to the initial safe set $\mathcal{A}_2$, the outputs do not seem to yield any activation/deactivation threshold for the production mechanism (i.e., the points in the space associated to an optimal control that commutes do not result in a specific curve).

Similarly, experiments performed by considering the safe set $\mathcal{A}_3$, defined on the food coordinate as per (10), did not show any particular threshold for the optimal controls, thus suggesting that a condition along that coordinate may not be the actual discriminant for the subtilin production mechanism.

These observations stress that, as expected, a meaningful outcome of the proposed interpretation and associated technique critically hinges on a correct choice of the survival function. For the problem under study and the developed dynamical model, the survival criterion in (8) has produced the most reasonable outcomes.

5. Conclusions and Future Work

This article suggests that the problem of survival of an organism, whose dynamics are described by a quantitative model, can be investigated via a safety analysis study, and that the strategies related to this problem can be

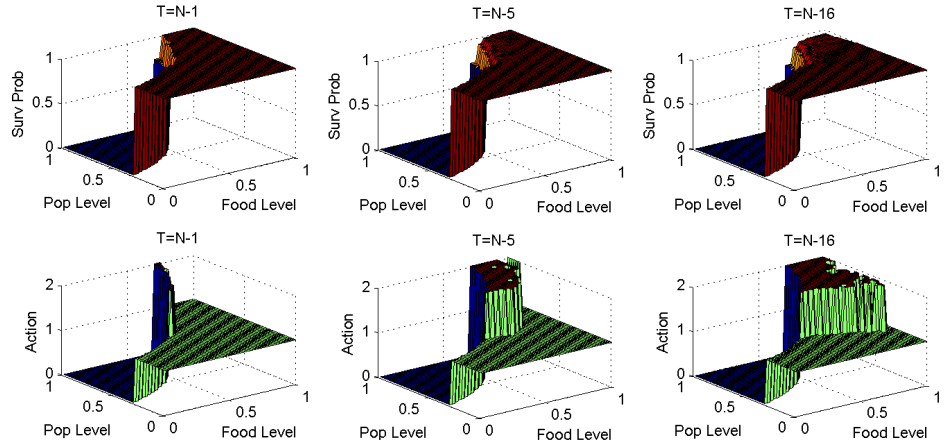

Figure 6: Maximal probabilistic safety level sets (top plots) and optimal controls (bottom plots), backwards in time (from left to right), based on a survival condition encoding competition in the environment. The horizontal coordinates denote nutrient and population level, whereas the vertical coordinate respectively survival probability (top) and optimal control (bottom).

synthesized by an optimal control approach. The mathematical framework of Stochastic Hybrid Systems, which is proposed in this work and formalized in [1], is endowed with generality and can be potentially applied to numerous other models in the literature.

For the specific study of the production mechanisms of the antibiotic subtilin as a stress-related response elicited by *Bacillus subtilis*, the argument developed in this work leads to conclude that the observed activation/deactivation mechanism displays a threshold feature over the state space, which is expected from the literature. This behavior is specifically associated with a condition on the organism and its environment, which is to be interpreted in terms of a particular level of its survival probability.

The wider applicability of the present study and the validity of the concept of optimality must of course raise a few caveats worthy of attention. Clearly, this approach subsumes the ability to define a meaningful survival function (and a corresponding safety region) for the system under study. In general, the figures of merit related to survival in (8), (9), and (10) ought to incorporate some energy-related term at the cellular level. Since we are interested in focusing on the possible presence of thresholds to be associated with the switching production mechanisms, rather than in the understanding their complete structure, this limitation plays a second role in the present contribution. However, it is critical to understand that a wrong choice for

this function may result in misleading conclusions, as discussed in Section 4.

From a biological perspective, it is necessary to understand what the exogenous "signals" are that the organism is able to sense, and which signals can presumably build up the survival function. Our choice of an average feedback signal from the environment may not be valid in general. Furthermore, the present study assumes that each cell independently maximizes its survival chances, thus ruling out any possible cooperative behavior.

As an extension to the present work, it would be instructive to understand what is the *critical* safety level that corresponds to the activation and the deactivation of the production of subtilin. Considering a more complex stress response network is also desirable, provided this trades off properly with the computational overhead and that modeling generality does not hide the understanding of the particular function under study. Furthermore, the use of randomized control structures, as suggested in other biological work [29], may make biological sense and can be accommodated within the presented SHS framework [1]. Finally, an ad hoc experimental study could actually verify the correctness of the predictions for the activation thresholds obtained by the presented methodology.

References

[1] A. Abate, M. Prandini, J. Lygeros, and S. Sastry. Probabilistic reachability and safety for controlled discrete time stochastic hybrid systems. *Automatica*, 44(11):2724–2734, Nov 2008.

[2] U. Alon. *An Introduction to Systems Biology: design principles of biological circuits*. Chapman and Hall/CRC Press, 2007.

[3] A. Arkin and J. Doyle. Appreciation of the machinations of the blind watchmaker. *IEEE Transactions on Circuits and Systems I – IEEE Transactions on Automatic Control*, pages 8–9, 2008. Special issue on Systems Biology.

[4] S. Banerjee and J. Hansen. Structure and expression of a gene encoding the precursor of subtilin, a small proteic antibiotic. *Journal of Biological Chemistry*, 263-19:9508–9514, 1988.

[5] G. Batt, D. Ropers, H. de Jong, J. Geiselmann, M. Page, and D. Schneider. Qualitative analysis and verification of hybrid models of genetic regulatory networks: Nutritional stress response in Escherichia coli. In

M. Morari and L. Thiele, editors, *Hybrid Systems: Computation and Control*, LNCIS 3414, pages 134–150. Springer Verlag, 2005.

[6] C.G. Cassandras and J. Lygeros. *Stochastic hybrid systems*. Automation and Control Engineering Series 24. Taylor & Francis Group/CRC Press, 2006.

[7] K.H. Cho, K.H. Johansson, and O. Wolkenhauer. A hybrid systems framework for cellular processes. *BioSystems*, 80:273–282, 2005.

[8] E. Cinquemani, R. Porreca, G. Ferrari-Trecate, and J. Lygeros. Subtilin production by *Bacillus subtilis*: Stochastic hybrid models and parameter identification. *IEEE Transactions on Circuits and Systems I – IEEE Transactions on Automatic Control*, pages 38–50, 2008. Special issue on Systems Biology.

[9] H. De Jong. Modeling and simulation of genetic regulatory systems: A literature review. *Journal of Computational Biology*, 9(1):67–103, 2002.

[10] J. Duprè. *The Latest on the Best: Essays on Evolution and Optimality*. MIT Press, Cambridge, MA, 1987.

[11] R. Ghosh, A. Tiwari, and C.J. Tomlin. Approximate symbolic reachability analysis with application to delta-notch signaling automata. In O. Maler and A. Pnueli, editors, *Hybrid Systems: Computation and Control*, Lecture Notes in Computer Science 2623, pages 233–248. Springer Verlag, 2003.

[12] J. Hu, W.-C. Wu, and S. Sastry. Modeling subtilin production in bacillus subtilis using stochastic hybrid systems. In R. Alur and G. J. Pappas, editors, *Hybrid Systems: Computation and Control*, Lecture Notes in Computer Science 2993, pages 417–431. Springer Verlag, 2004.

[13] E. Katz and A.L. Demain. The peptide antibiotics of *Bacillus*: Chemistry, biogenesis, and possible functions. *Bacteriological Reviews*, 41(2):449–474, June 1977.

[14] P. Kiesau, U. Eikmanns, Z. Eckel, S. Weber, M. Hammelmann, and K. Entian. Evidence for a multimeric subtilin synthetase complex. *Journal of Bacteriology*, 179-5:1475–1481, 1997.

[15] C. Klein and K. Entian. Genes involved in self-protection against the lantibiotic subtilin produced by *Bacillus subtilis* atcc 6633. *Applied and Environmental Microbiology*, 60(8):2793–2801, 1994.

[16] P. Lincoln and A. Tiwari. Symbolic systems biology: hybrid modeling and analysis of biological networks. In R. Alur and G. J. Pappas, editors, *Hybrid Systems: Computation and Control*, Lecture Notes in Computer Science 2993, pages 660–672. Springer Verlag, 2004.

[17] J. Maynard Smith. *Evolution and the Theory of Games*. Cambridge University Press, New York, 1982.

[18] S. Mehra, S. Charaniya, E. Takano, and W.-S. Hu. A bistable gene switch for antibiotic biosynthesis: The butyrolactone regulon in *Streptomyces coelicolor*. *PLoS ONE*, 3(8):e2724, 2008.

[19] T. Msadek. When the going gets tough: survival strategies and environmental signaling networks in *bacillus subtilis*. *Trends in Microbiology*, 7(5):201–207, 1999.

[20] C. Rao and A. Arkin. Control motifs for intracellular regulatory networks. *Annu. Rev. Biomed. Eng.*, pages 391–419, 2001.

[21] R. Rosen. *Optimality Principles in Biology*. Plenum Press, New York, 1967.

[22] F. Schueller, R. Benz, and H.G. Sahl. The peptide antibiotic subtilin acts by formation of voltage-dependent multi-stage pores in bacterial and artificial membranes. *European Journal of Biochemistry*, 182:181–186, 1989.

[23] D. Segre, D. Vitkup, and G.M. Church. Analysis of optimality in natural and perturbed metabolic networks. *PNAS*, 99-33:15112–15117, 2002.

[24] T. Stein. *Bacillus subtilis* antibiotics: structures, syntheses and specific functions. *Molecular Microbiology*, 56-4:845–857, 2005.

[25] T. Stein, S. Borchert, P. Kiesau, S. Heinzmann, S. Kloss, C. Klein, M. Helfrich, and K. Entian. Dual control of subtilin biosynthesis and immunity in *bacillus subtilis*. *Molecular Microbiology*, 44-2:403–416, 2002.

[26] T. Stein, S. Heinzmann, S. Düsterhus, S. Borchert, and K. Entian. Expression and functional analysis of the subtilin immunity genes *spaIFEG* in the subtilin-sensitive host *Bacillus subtilis* mo1099. *Bacteriology*, 187(3):822–828, 2005.

[27] T. Stein, S. Heinzmann, P. Kiesau, B. Himmel, and K. Entian. The *spa*-box for transcriptional activation of subtilin biosynthesis and immunity in *Bacillus subtilis*. *Molecular Microbiology*, 47(6):1627–1836, 2003.

[28] H. Tjalsma, E. Koetje, R. Kiewet, O. Kuipers, M. Kolman, J. van der Laan, R. Daskin, E. Ferrari, and S. Bron. Engineering of quorum-sensing systems for improved production of alkaline protease by *bacillus subtilis*. *Journal of Applied Microbiology*, 96:569–578, 2004.

[29] D. Wolf, V. Vazirani, and A.Arkin. Diversity in times of adversity: probabilistic strategies in microbial survival games. *J. theor. biol.*, 234(2):227–253, 2005.